

Evaluation of image quality on low contrast media with deep learning image reconstruction algorithm in prospective ECG-triggering coronary CT angiography

Dian Yuan

The First Affiliated Hospital of Zhengzhou University

Luotong Wang

GE Healthcare China

Peijie Lyu

The First Affiliated Hospital of Zhengzhou University

Yonggao Zhang

The First Affiliated Hospital of Zhengzhou University

Jianbo Gao

The First Affiliated Hospital of Zhengzhou University

Jie Liu (✉ liujjeict@163.com)



The First Affiliated Hospital of Zhengzhou University

Research Article

Keywords: Computed Tomography Angiography, Contrast Medium, Coronary Vessels

Posted Date: December 7th, 2023

DOI: <https://doi.org/10.21203/rs.3.rs-3704717/v1>

License:   This work is licensed under a Creative Commons Attribution 4.0 International License. [Read Full License](#)

Additional Declarations: No competing interests reported.

Abstract

Purpose To assess the impact of low-dose contrast medium (CM) injection protocol with deep learning image reconstruction (DLIR) algorithm on image quality in coronary CT angiography (CCTA).

Methods and Materials 210 patients undergoing CCTA were prospectively and randomly assigned to three groups with different contrast volume protocols (at 320mgI/mL concentration and constant flow rate of 5ml/s): Group A, 0.7mL/kg (n = 70); Group B, 0.6mL/kg (n = 70); Group C, 0.5mL/kg (n = 70). All patients were examined via a prospective ECG-triggered scan protocol within one heartbeat. A high level DLIR (DLIR-H) algorithm was used for image reconstruction with a thickness and interval of 0.625mm. The CT values of ascending aorta (AA), descending aorta (DA), three main coronary arteries, pulmonary artery (PA), and superior vena cava (SVC) were measured and analyzed for objective assessment. Two radiologists assessed the image quality and diagnostic confidence using a 5-point Likert scale.

Results The CM doses were 46.81 ± 6.41 mL, 41.96 ± 7.51 mL and 34.65 ± 5.38 mL for Group A, B and C, respectively. The objective assessments on AA, DA and the three main coronary arteries and the overall subjective scoring showed no difference among the three groups (all $p > 0.05$). Group A had higher enhancements in PA and SVC than groups B and C (all $p < 0.05$).

Conclusions CCTA reconstructed with DLIR could be realized with adequate enhancement in coronary arteries, excellent image quality and diagnostic confidence at low contrast dose of 0.5mL/kg. The use of lower tube voltages may further reduce the contrast dose requirement.

Introduction

In the clinical examination of coronary artery disease (CAD), Coronary computed tomography angiography (CCTA) provides a non-invasive examination method with high diagnostic accuracy, high sensitivity, and high specificity[1, 2]. Studies have indicated that the high dose of contrast medium (CM) contributed significantly to the diagnostically acceptable CCTA[3, 4]. However, high CM dose on patients with poor glomerular filtration rate would more likely cause contrast-induced nephropathy (CIN) [5–8]. Therefore, the use of low CM in CCTA have significant clinical value, especially in patients with renal failure.

Attempts have been made to reduce the CM dose without compromising the CCTA image quality [9–13], such as wide-coverage detectors which could shorten the acquisition time of CCTA, therefore, leading to lower CM.

Nowadays, continuous development of image reconstruction algorithms can achieve low radiation dose and low CM while maintaining good image quality [14]. In recent decades, Filtered back projection (FBP) and iterative reconstruction (IR) algorithms have been the mainstream CCTA reconstruction algorithms. FBP algorithm is a spatial processing technique based on the Fourier transform theory. Unlike conventional FBP, which uses linear mathematical operations, IR algorithms use nonlinear operations to significantly reduce image noise. However, plastic-like or wax-like images often appear after using high-strength IR algorithms under low radiation dose conditions. Deep learning image reconstruction (DLIR, TrueFidelity, GE Healthcare)

algorithm, which uses high-quality FBP images as the reference and extracts multiple critical features by the integrated complex architecture, has showed the ability to overcome limitations of FBP and IR. Phantom and clinical studies[9, 10, 14–17] have shown that DLIR could improve image quality by reducing noise and maintaining image texture.

Several studies[9, 10] suggested that low tube voltage combined with DLIR can achieve low radiation dose and low CM in CCTA. However, as far as we know, few studies evaluated the clinical values of only CM dose reduction in combination with DLIR, especially considering patients with a wide range heart rates (HRs) prescribed with CCTA. Therefore, the purpose of our study was to assess the optimized contrast medium CCTA protocol assisted by DLIR in patients with wide range heart rates (HRs).

Materials and Methods

Study population

The local ethics committee approved this prospective study, and all participants provided informed consent forms.

Between March and July 2023, 231 participants with suspected CAD were prospectively considered for enrollment in the study. Participants with the following characteristics were excluded: (1) known iodine contrast medium allergy, (2) renal insufficiency, (3) respiratory disorders, (4) previous coronary artery bypass grafting, (5) clinical instability or significant heart failure (Fig. 1). Finally, 210 participants were enrolled and randomly assigned to three groups to undergo CCTA with three different contrast medium dose protocols: Group A (n = 70), 0.7 mL/kg CM; Group B (n = 70), 0.6 mL/kg CM; Group C (n = 70), 0.5 mL/kg CM. Participants' sex, age, weight, BMI, and HR were recorded.

We paired the patients based on the basic information. A subgroup analysis based on patient heart rate (HR) was also performed, where $HR \leq 66$ bpm was the low HR group and $HR > 66$ bpm was the high HR group.

Image acquisition

All patients underwent CCTA scans on a new 256-row, 16 cm wide-detector CT scanner (Revolution Apex CT, GE HealthCare, USA). Image acquisition parameters were consistent among the three groups: prospectively ECG-triggered CCTA mode; tube voltage of 100 kV; noise index (NI) of 12 HU (mA range: 300–1200); gantry rotation time of 0.28s. Coronary opacification was monitored at the ascending aorta slice at the level of the left main pulmonary artery, and the trigger threshold was set at 100 Hounsfield units (HU). The breath-holding technique was used to minimize the respiration-related motion artifacts. Besides, all scanning was performed with the automatic tube current modulation technique, ranging from 300mA to 1200mA (Smart mA). The detector z-coverage size was selected to be 120 mm, 140 mm, or 160 mm according to the patients' heart sizes. The auto-gating technique was used to acquire projections at the ideal cardiac phases (R-R interval) based on patients' HR before the scanning: 70–80% of the R-R interval for patients with $HR < 65$ bpm; 40–80% for patients with HR ranging from 66 to 85 bpm; and 40–55% for patients with $HR > 86$

bpm. The data acquisition for the whole heartbeat cycle (0-100% R-R interval) was obtained for patients with arrhythmia (heart rate varies more than ten bpm).

All participants took 0.5 mg of nitroglycerin sublingually before the examination to induce vasodilation. To ensure unobstructed contrast flow, 18 mL of 0.9% saline injected at a flow rate of 5 mL/s was used for test. For all groups, pre-warmed CM (iodixanol, 320 mgI/ mL, Visipaque, General Electric Company, USA) was injected through the anterior cubital vein via an 18-gauge catheter at a flowrate of 5 mL/s with a double-syringe power injector (Ulrich Medical, XD 2040, China). The injection protocol of CM was personalized to patient weight by applying 0.7 mL/kg for Group A, 0.6 mL/kg for Group B, and 0.5 mL/kg for Group C. Finally, 40 mL of saline chaser was injected at the same flow rate.

CCTA images were reconstructed using the high level of deep learning image reconstruction algorithm (DLIR-H) with thickness and interval of 0.625mm, a pixel matrix size of 512 × 512, with the field of view for reconstruction adapted to the size of each participant and the newest snapshot freeze technique (SSF2, GE HealthCare) was used to correct motion artifacts.

Deep learning image reconstruction algorithm

The commercial DLIR algorithm (TrueFidelity, GE HealthCare) [9, 10] was built based on the CT vendor's detailed design embedded in a convolutional neural network. The algorithm took a chest CT sinogram as input data, and the ground truth was standard-dose CT information reconstructed by filtered back projection (FBP) of the same patient. The ground truth training data are images from both phantoms and patients. The DLIR algorithm was deployed to run on the reconstruction hardware of a specific CT system.

Objective assessment

All images were transferred to a post-processing workstation (AW4.7, GE HealthCare, USA) to generate volume rendering (VR), maximum intensity projection (MIP), curved planar reformat (CPR), and multi-planar reformations (MPR) for subjective and objective image quality evaluation and comparison.

A cardiologist with 11-year experience, blinded to the experiment assignment, performed the objective assessments. Regions of interest (ROIs) were placed in ascending aorta (AA), descending aorta (DA), pulmonary artery (PA), superior vena cava (SVC), right atrium (RA), right ventricle (RV), left atrium (LA), left ventricle (LV), coronary vein (CV) and proximal, middle and distal segment of the three main coronary arteries, which were left anterior descending (LAD), left circumflex (LCX) and right coronary artery (RCA). ROIs for AA, DA, PA, and SVC were placed at the level of the pulmonary artery bifurcation, and ROIs for RA, RV, LA, and LV were placed at the level of the four-chambered heart. The sizes of the circular ROI cursors were drawn as large as possible according to the vascular internal diameter. During the placement of ROIs, researchers paid close attention to avoiding vessel walls, plaques[19], artery stents, calcification and streak artifacts[20]. The measurement at each vessel position was obtained by averaging over three consecutive slices. Signal-to-noise ratio (SNR) and contrast-to-noise ratio (CNR) were calculated using the following formulas:

$$SNR = \frac{CT_{vessel}}{SD_{vessel}}$$

$$CNR = \frac{CT_{vessel} - CT_{myocardium}}{SD_{vessel}}$$

Therein, CT vessel indicates CT attenuation of vascular lumen; SD vessel points to standard deviation of attenuation of vascular lumen; CT myocardium indicates the attenuation of the left ventricular wall, measured at the level of the four-chamber heart.

Subjective assessment

For subjective scoring, images were displayed randomly and unmarked to two observers with 11 and 23 years of experience in CT cardiovascular imaging. Unaware of the group allocation, clinical indications and imaging findings, these observers independently evaluated the image sharpness and diagnostic confidence. They were allowed to freely adjust the window level and width when assessing vascular opacity. Qualitative image quality was scored using 5-point Likert scale as follows[18, 19]: 5, excellent (no artifact, clearly displayed lumen, clear delineation of the vessel walls and complete diagnosis); 4, good (slight artifact, good delineation of vessel walls and basic diagnosis); 3, moderate (moderate artifact, moderate delineation of vessel walls and approximate diagnosis); 2, poor (prominent artifact and structure discontinuity, poor delineation of vessel walls and less diagnosis); 1, non-diagnostic (severe artifact, poor vessel wall definition and non-diagnosis).

Radiation dose estimates

The volumetric CT dose index (CTDI_{vol}) and the dose length product (DLP) were recorded from the dose report. The effective radiation dose (ED) was estimated by multiplying the DLP by the cardiac conversion coefficient ($k = 0.014 \text{mSv} \times \text{mGy}^{-1} \times \text{cm}^{-1}$)[13, 20].

Statistical analysis

Statistical analyses were performed using SPSS (IBM, version 25.0, USA). Normally distributed quantitative data were expressed as mean \pm standard deviation and tested by one-way analysis of variance (Bonferroni correction was used for post hoc tests), and data with non-normal distributions were expressed as medians and interquartile ranges and tested by Kruskal-Wallis H (Mann Whitney U was used for post hoc tests). Categorical variables of the two groups were compared using the chi-squared test. For subjective image quality, our study assessed the inter-reader agreement between two observers with Cohen's kappa where kappa values < 0 were considered as indicating no agreement, $0.0 < k \leq 0.2$ as poor, $0.2 < k \leq 0.4$ as fair, $0.4 < k \leq 0.6$ as moderate, $0.6 < k \leq 0.8$ as substantial, and $0.8 < k \leq 1.0$ as excellent agreement. The difference in each reader's rating across groups was tested by the Chi-square analysis. A p-value of 0.05 or less was considered statistically significant.

Results

Patients' basic information

The baseline characteristics and radiological parameters of the included participants are shown in Table 1. There was no statistical difference in the demographics and radiation doses among Group A, Group B and

Group C (all $p > 0.05$) (Table 1). Compared with Group A, the total amount of CM in Group B and Group C was reduced by 10.4% and 23.9%, respectively.

Table 1
Baseline patient characteristics and scanning parameters.

Variables	Group A (n = 70)	Group B (n = 70)	Group C (n = 70)	P value
Age (years) *	54.21 ± 11.60	58.11 ± 12.09	54.21 ± 14.79	0.121
Gender				0.780
Female	31 (44.3%)	35 (50.0%)	32 (45.7%)	
Male	39 (55.7%)	35 (50.0%)	38 (54.3%)	
Height (m) *	1.65 ± 0.08	1.65 ± 0.08	1.66 ± 0.08	0.856
Weight (kg) *	66.87 ± 9.15	69.94 ± 12.52	69.3 ± 10.76	0.216
BMI (kg/m ²) *	24.41 ± 2.85	25.51 ± 3.27	25.14 ± 3.12	0.105
Heart Rate (bpm) *	74.29 ± 29.18	72.67 ± 18.59	70.00 ± 15.45	0.505
Tube Voltage (kV)	100	100	100	1.000
Tube Current (mAs) *	953.56 ± 74.63	963.70 ± 57.2	975.69 ± 12.45	0.059
CM Dose(mL/kg)	0.7	0.6	0.5	< 0.001
CM flow rate (mL/s)	5	5	5	1.000
CM volume(mL) *	46.81 ± 6.41 ^{b,c}	41.96 ± 7.51 ^{a,c}	34.65 ± 5.38 ^{a,b}	< 0.001
CTDI _{vol} (mGy) *	8.71 ± 1.63	8.25 ± 1.46	8.86 ± 1.89	0.084
DLP (mGy·cm) *	126.55 ± 23.46	122.71 ± 22.19	129.43 ± 27.35	0.266
ED (mSv) *	1.77 ± 0.33	1.72 ± 0.31	1.81 ± 0.38	0.264
Note.—Data in parentheses are percentages.				

* Data are means ± standard deviation.

a Statistical significance with group A, $p < 0.05$

b Statistical significance with group B, $p < 0.05$

c Statistical significance with group C, $p < 0.05$

Image quality assessment

Both the objective assessment and the subjective assessment proved that the 10.4% contrast reduction protocol and the 23.9% contrast reduction protocol could achieve similar images with the normal contrast protocol (Fig. 2, Table 2). Specifically, the vascular CT attenuation, SNR and CNR of all coronary arteries did

not show statistical differences among the three groups (all $p < 0.05$), and the CT values of myocardium also did not show statistically different (Table 2). No statistical differences were found between the two observers' subjective assessments of the three groups ($p = 0.929$, $p = 0.974$). The difference in subjective image quality rating between two observers never exceeded one point, and their evaluations reached a Cohen's kappa of 0.796 (95% CI: 0.700-0.892) (Fig. 3).

Table 2
Objective image quality assessment in coronary arteries and myocardium

Parameter	location	Group A	Group B	Group C	P value
Vascular attenuation (HU), (mean ± SD)	pLAD	472.11 ± 71.81	464.68 ± 54.30	453.02 ± 57.74	0.185
	mLAD	416.29 ± 59.17	402.87 ± 45.59	401.51 ± 45.77	0.164
	dLAD	355.99 ± 48.90	345.28 ± 29.02	344.49 ± 27.43	0.116
	pRCA	473.46 ± 62.24	469.41 ± 61.85	450.27 ± 57.44	0.056
	mRCA	427.10 ± 49.39	421.86 ± 53.48	415.50 ± 58.26	0.444
	dRCA	365.43 ± 43.77	353.81 ± 39.03	352.82 ± 34.45	0.110
	pLCX	462.44 ± 66.72	460.92 ± 59.52	443.90 ± 51.54	0.127
	mLCX	411.15 ± 56.55	409.43 ± 56.63	402.02 ± 47.36	0.565
	dLCX	347.91 ± 42.28	345.78 ± 30.05	344.65 ± 34.79	0.863
	Myocardium	83.28 ± 15.19	82.27 ± 19.01	81.92 ± 16.01	0.883
SNR (mean ± SD)	pLAD	30.08 ± 8.30	29.73 ± 9.10	28.84 ± 10.1	0.710
	mLAD	22.99 ± 7.13	22.65 ± 6.68	21.75 ± 5.90	0.517
	dLAD	20.07 ± 7.13	19.85 ± 7.13	19.72 ± 6.60	0.957
	pRCA	28.77 ± 8.60	29.75 ± 9.71	27.31 ± 6.48	0.223
	mRCA	25.84 ± 10.43	23.97 ± 8.96	22.92 ± 6.56	0.141
	dRCA	19.52 ± 6.87	19.65 ± 5.86	19.46 ± 6.28	0.985
	pLCX	28.64 ± 9.87	28.21 ± 8.05	26.03 ± 9.42	0.195
	mLCX	22.64 ± 8.23	22.58 ± 6.59	22.56 ± 7.03	0.998
	dLCX	20.60 ± 7.80	20.51 ± 5.75	19.74 ± 5.68	0.691
CNR (mean ± SD)	pLAD	24.96 ± 7.32	24.49 ± 7.74	23.73 ± 8.50	0.649
	mLAD	18.52 ± 5.96	18.01 ± 5.38	17.43 ± 4.91	0.497
	dLAD	15.52 ± 5.60	15.16 ± 5.65	15.16 ± 5.1	0.903
	pRCA	23.89 ± 7.50	24.59 ± 8.41	22.46 ± 5.58	0.212

Parameter	location	Group A	Group B	Group C	P value
	mRCA	20.96 ± 8.61	19.33 ± 7.65	18.48 ± 5.34	0.129
	dRCA	15.29 ± 5.85	15.10 ± 4.69	15.10 ± 5.03	0.970
	pLCX	23.73 ± 8.69	23.20 ± 6.93	21.36 ± 7.84	0.174
	mLCX	18.24 ± 6.96	18.06 ± 5.63	18.10 ± 5.83	0.984
	dLCX	15.84 ± 6.26	15.64 ± 4.46	15.16 ± 4.45	0.721

Note.— dLAD = proximal, middle, and distal portions of the left anterior descending coronary artery, respectively; pLCX, mLCX, and dLCX = proximal, middle, and distal portions of the left circumflex artery, respectively; pRCA, mRCA, and dRCA = proximal, middle, and distal portions of the right coronary artery, respectively; SNR = Signal to noise ratio; CNR = contrast to noise ratio; HU = Hounsfield Unit; IQR = interquartile range; SD = standard deviation.

Vascular attenuation with standard deviations in each measurement location, SNR and CNR with interquartile range.

We also noticed that the CT values of AA and DA showed no statistical difference (all $p > 0.05$). However, the CT values for SVC, PA, LA, LV, RA, RV, and CV were significantly different in three groups (all $p < 0.05$), and the CT values of these vessels are decreasing in order: Group A > Group B > Group C (Fig. 4). Representative cases of three groups are shown in Fig. 5.

Subgroup analysis

Furthermore, we conducted comparison for high HR patients and normal HR patients by separating our patients in three groups into the high HR group ($HR > 66\text{bpm}$) and the normal HR group ($HR \leq 66\text{bpm}$). There were no significant differences in intracoronary attenuation values between the higher HR subgroup and the lower HR subgroup among three groups (all $p > 0.05$) (Table 3, Fig. 6), which demonstrates that the low contrast regimen we proposed in this study was applicable to patients of any HR.

Table 3
Comparison of CT attenuation between CCTA images for patients with different HR.

CT Value (HU)	Group A			Group B			Group C		
	Lower HR	Higher HR	P value	Lower HR	Higher HR	P value	Lower HR	Higher HR	P value
	(HR ≤ 66, n = 34)	(HR > 66, n = 36)		(HR ≤ 66, n = 28)	(HR > 66, n = 42)		(HR ≤ 66, n = 34)	(HR > 66, n = 36)	
pLAD	473.46 ± 66.99	470.83 ± 77.01	0.880	456.46 ± 56.97	471.21 ± 51.89	0.262	447.88 ± 56.42	457.87 ± 59.35	0.474
mLAD	421.45 ± 56.16	411.42 ± 62.27	0.482	392.09 ± 48.18	411.44 ± 42.09	0.078	397.27 ± 47.29	405.51 ± 44.58	0.456
dLAD	359.09 ± 44.69	353.06 ± 53.03	0.609	340.64 ± 27.00	348.97 ± 30.37	0.236	348.08 ± 30.63	341.10 ± 23.96	0.294
pLCX	463.49 ± 65.33	461.44 ± 68.93	0.899	456.46 ± 65.87	464.45 ± 54.57	0.581	438.64 ± 55.39	448.87 ± 47.87	0.411
mLCX	419.92 ± 59.54	402.87 ± 53.07	0.210	406.17 ± 64.66	412.03 ± 50.07	0.670	397.56 ± 43.56	406.23 ± 50.95	0.449
dLCX	350.71 ± 47.21	345.27 ± 37.52	0.596	340.68 ± 29.61	349.84 ± 30.16	0.208	342.05 ± 33.90	347.11 ± 35.91	0.547
pRCA	466.34 ± 60.30	480.19 ± 64.14	0.356	462.77 ± 69.02	474.70 ± 55.86	0.427	449.50 ± 58.53	450.99 ± 57.22	0.914
mRCA	432.51 ± 48.20	422.00 ± 50.63	0.377	416.00 ± 57.77	426.52 ± 50.09	0.417	405.35 ± 50.09	425.09 ± 64.27	0.158
dRCA	370.24 ± 45.23	360.88 ± 42.47	0.375	350.09 ± 42.41	356.77 ± 36.42	0.481	350.33 ± 33.24	355.17 ± 35.86	0.560
Myocardium	82.84 ± 14.81	83.70 ± 15.73	0.816	79.70 ± 19.62	84.32 ± 18.52	0.316	79.89 ± 15.98	83.83 ± 16.02	0.306

Note.—Unless otherwise specified, data are means ± standard deviation. dLAD = proximal, middle, and distal portions of the left anterior descending coronary artery, respectively; pLCX, mLCX, and dLCX = proximal, middle, and distal portions of the left circumflex artery, respectively; pRCA, mRCA, and dRCA = proximal, middle, and distal portions of the right coronary artery, respectively

Discussion

In this study, we evaluated the feasibility of a using low-contrast dose protocol in CCTA assisted by DLIR algorithm. Our results proved that the 24% contrast reduction protocol (0.5 mL/kg) could achieve similar images to the standard contrast protocol. Moreover, the low contrast dose protocol we proposed in this study could be applied to patients with both average HR and high HR.

With the advancement of technology, acquisition time of CCTA has become shorter, and the injection time of contrast medium is also shortened, so the contrast medium dose injection should also be reduced. As a

result, there is a clinical trend to reduce the amount of contrast medium[8–10]. However, how to balance image quality and contrast dose is difficult and is the focus of many studies. Our results showed that good image quality could still be obtained when the contrast dose was reduced by 24%, which can greatly reduce the risk of contrast-related diseases such as CIN.

We have noticed that significant efforts have been made to reduce the CM for CCTA. Andreini et al. [20] tried to reduce the CM to 50 mL at 400 mgI/mL for normal-size patients ($BMI < 24.9 \text{ kg/m}^2$) and for over-weighted patients ($BMI \geq 25 \text{ kg/m}^2$). In our study, we personalized the CM injection protocol for patients with an extensive range of body size. Notably, in our study, if the CM was 50mL, the patient's BMI would be 25 kg/m^2 , which would be injected 60mL in the study of Andreini et al. Thus, the CM dosage in our study was much lower than the study of Andreini et al. Furthermore, Wang et al. [14] have tried lower CM protocol to 35mL with 70kVp for normal patients ($BMI \leq 26 \text{ kg/m}^2$) and 40mL with 80kVp for over-weight patients ($BMI > 26 \text{ kg/m}^2$). However, despite using the 100kVp in our study, our study still used less contrast dose in terms of mg-iodine since the contrast medium in Wang's study had a concentration of 400 mgI/mL, while the one used in our study was 320 mgI/mL. Let us assume an overweight patient who was 1.8m and 90kg ($BMI = 27.78 \text{ kg/m}^2$), then he would require 16g iodine ($40 \text{ mL} \times 400 \text{ mgI/mL}$) as described in the study of Wang et al. but only 14.4g ($90 \text{ kg} \times 0.5 \text{ mL/kg} \times 320 \text{ mgI/mL}$) iodine in our study. Furthermore, let us assume a normal patient who was 1.7m and 65kg ($BMI = 22.49 \text{ kg/m}^2$), then he would use 14g ($35 \text{ mL} \times 400 \text{ mgI/mL}$) iodine in the study of Wang et al. and 10.4g iodine ($65 \text{ kg} \times 0.5 \text{ mL/kg} \times 320 \text{ mgI/mL}$) in our study. We believe we could further reduce the CM dose if we use lower tube voltages in the future. Moreover, we noticed that the difference in vascular attenuation between the two groups was greater than 100HU in the study of Wang et al. In contrast, our contrast protocol with controlled injection time could ensure the consistency of vascular attenuation values at different CM doses. Besides, we assessed the objective scores for both the major vessels and the myocardium compared with the studies of Wang et al. and Li et al. [10, 14].

One of the interesting or even controversy phenomena we observed in our study was that similar degrees of enhancement were obtained for coronary vessels and myocardium among the three imaging groups, even though same tube voltage was used and two of the groups used contrast volumes as much as 24% less. On the other hand, the same conclusion could not be made for vessels such as pulmonary artery and superior vena cava. As it was shown in our results that CT values of PA, SVC, LA, LV, RA, RV and CV in Group A were higher than the other two low-CM groups (all $p < 0.001$, Fig. 4). One of the explanations could be that a large amount of contrast was stuck in these vessels at the time of CCTA acquisition, and the additional contrast volume in Group A did not contribute to the imaging in CCTA and the overbrightness of the superior vena cava may also affect our diagnosis of coronary images. Therefore, the 24% contrast reduction protocol was still sufficient to provide adequate enhancement in coronary arteries.

Furthermore, we have conducted subgroups analysis based on HR and we proved that the low contrast dose protocol we proposed in this study could be applied to patients with both average HR and high HR. High HR has been criticized for degraded image quality in CCTA examination, which has raised a significant concern[21–24] in recent years. Compared to patients with regular HR, CCTA images of patients with high heart rates suffer from motion artifacts due to their uneven ratio of systolic to diastolic phases and their

excessive motion velocities that exceed the temporal resolution of the CT scanners. In our study, all patients were examined on a new 256-row, 16-cm-wide detector CT scanner with a rotational speed of 280 ms for examinations within a single heartbeat prospective ECG-triggered scan protocol, which took good advantage of the detector's wide coverage and fast rotation speed to significantly reduce the adverse effects of high HR on CCTA image quality. Additionally, this study used the SmartPhase technique to automatically select the optimal reconstruction phase with the SSF2 motion correction algorithm, which could significantly reduce motion artifacts in CCTA images of patients with high HR. Moreover, we have assessed the CT value of the myocardium and our results showed that the myocardium could also be well enhanced with the low CM scanning protocols. CT values of the major vessels and myocardium were consistent in patients with normal HR and high HR.

DLIR is an artificial intelligence reconstruction technique, which integrates high quality FBP images and extracts more key features of the same image. This algorithm can solve the problem that the use of FBP or high intensity IR in low tube voltage CT scans may be either too noisy or affecting the image texture[25, 26]. Previous studies[9, 10, 14–17] have shown that DLIR has more potential to improve image quality and reduce image noise at the same radiation dose and tube voltage. Consistent with previous studies, our study also demonstrated that the excellent diagnostic images of CCTA were acquired with DLIR-H algorithm.

This study has several limitations. First, the sample size of the study was limited. Second, a conventional tube voltage of 100 kV was used in this study, not the lower tube voltages which could further reduce the CM dose. However, we believe the use of 100 kV should not change the basic conclusion that contrast dose could be optimized in CCTA. Third, we did not apply the free-breathing technique in our study, but the use of breath-holding was intended to minimize motion artifacts, and future studies will attempt to allow patients to breathe freely for CCTA examinations. Finally, this contrast protocol has not been validated on other CT scanners. Further study could be established on various CT scanners, using our low-CM protocol as a reference.

In conclusion, contrast medium dose may be reduced by 24% to 0.5 mL/kg (at concentration of 320 mgI/mL) in CCTA to maintain adequate enhancement in coronary arteries. reduction protocol assisted with DLIR could achieve good CCTA image quality in patients with an extensive range of heart rates.

Abbreviations

AA (ascending aorta)

ASIR (adaptive statistical iterative reconstruction)

BMI (body mass index)

CAD (coronary artery disease)

CCTA (coronary CT angiography)

CIN (contrast-induced nephropathy)

CM (contrast medium)

CNR (contrast-to-noise ratio)

CPR (curved planar reformat)

CTDIvol (volume CT dose index)

CV (coronary vein)

DA (descending aorta)

DLIR (deep learning image reconstruction)

DLP (dose length product)

ED (effective dose)

FBP (filtered back-projection)

HR (heart rate)

IR (iterative reconstruction)

LAD (left anterior descending branch)

LA (left atria)

LCX (left circumflex branch)

LV (left ventricles)

MIP (maximum intensity projection)

MPR (multi-planar reformations)

NI (noise index)

PA (pulmonary artery)

RA (right atria)

RCA (right coronary artery)

ROI (regions of interest)

RV (right ventricles)

SNR (signal-to-noise ratio)

SVC (superior vena cava)

VR (volume rendering)

Declarations

Author Contribution

Dian Yuan: Formal analysis, Investigation, Data Curation, Writing - Original Draft, Writing - Review & Editing, Visualization
Luotong Wang: Data Curation, Formal analysis, Writing - Review & Editing
Peijie Lyu: Data Curation, Writing - Review & Editing
Yonggao Zhang: Data Curation
Jianbo Gao: Supervision
Jie Liu: Conceptualization, Supervision, Project administration

References

1. Knuuti J, Wijns W, Saraste A, Capodanno D, Barbato E, Funck-Brentano C, Prescott E, Storey RF, Deaton C, Cuisset T, Agewall S, Dickstein K, Edvardsen T, Escaned J, Gersh BJ, Svitil P, Gilard M, Hasdai D, Hatala R, Mahfoud F, Masip J, Muneretto C, Valgimigli M, Achenbach S, Bax JJ, Group ESCSD (2020) 2019 ESC Guidelines for the diagnosis and management of chronic coronary syndromes. *Eur Heart J* 41:407-477. <https://10.1093/eurheartj/ehz425.org/10.1093/eurheartj/ehz425>
2. Investigators S-H, Newby DE, Adamson PD, Berry C, Boon NA, Dweck MR, Flather M, Forbes J, Hunter A, Lewis S, MacLean S, Mills NL, Norrie J, Roditi G, Shah ASV, Timmis AD, van Beek EJR, Williams MC (2018) Coronary CT Angiography and 5-Year Risk of Myocardial Infarction. *N Engl J Med* 379:924-933. <https://10.1056/NEJMoa1805971.org/10.1056/NEJMoa1805971>
3. Zhang Q, Mi H, Shi X, Li W, Guo S, Wang P, Suo H, Wang Z, Jin S, Yan F, Niu Y, Xian J (2021) Higher Iodine Concentration Enables Radiation Dose Reduction in Coronary CT Angiography. *Acad Radiol* 28:1072-1080. <https://10.1016/j.acra.2020.05.012.org/10.1016/j.acra.2020.05.012>
4. Aschoff AJ, Catalano C, Kirchin MA, Krix M, Albrecht T (2017) Low radiation dose in computed tomography: the role of iodine. *Br J Radiol* 90:20170079. <https://10.1259/bjr.20170079.org/10.1259/bjr.20170079>
5. Barrios Lopez A, Garcia Martinez F, Rodriguez JI, Montero-San-Martin B, Gomez Rioja R, Diez J, Martin-Hervas C (2021) Incidence of contrast-induced nephropathy after a computed tomography scan. *Radiologia (Engl Ed)* 63:307-313. <https://10.1016/j.rxeng.2020.02.005.org/10.1016/j.rxeng.2020.02.005>
6. Eng J, Wilson RF, Subramaniam RM, Zhang A, Suarez-Cuervo C, Turban S, Choi MJ, Sherrod C, Hutfless S, Iyoha EE, Bass EB (2016) Comparative Effect of Contrast Media Type on the Incidence of Contrast-Induced Nephropathy: A Systematic Review and Meta-analysis. *Ann Intern Med* 164:417-424. <https://10.7326/M15-1402.org/10.7326/M15-1402>
7. Laville M, Juillard L (2010) Contrast-induced acute kidney injury: How should at-risk patients be identified and managed? *Journal of nephrology* 23:387-398.

8. Liu J, Gao J, Wu R, Zhang Y, Hu L, Hou P (2013) Optimizing contrast medium injection protocol individually with body weight for high-pitch prospective ECG-triggering coronary CT angiography. *Int J Cardiovasc Imaging* 29:1115-1120. <https://10.1007/s10554-012-0170-x.org/10.1007/s10554-012-0170-x>
9. Sun J, Li H, Li J, Cao Y, Zhou Z, Li M, Peng Y (2021) Performance evaluation of using shorter contrast injection and 70 kVp with deep learning image reconstruction for reduced contrast medium dose and radiation dose in coronary CT angiography for children: a pilot study. *Quant Imaging Med Surg* 11:4162-4171. <https://10.21037/qims-20-1159.org/10.21037/qims-20-1159>
10. Li W, Diao K, Wen Y, Shuai T, You Y, Zhao J, Liao K, Lu C, Yu J, He Y, Li Z (2022) High-strength deep learning image reconstruction in coronary CT angiography at 70-kVp tube voltage significantly improves image quality and reduces both radiation and contrast doses. *Eur Radiol* 32:2912-2920. <https://10.1007/s00330-021-08424-5.org/10.1007/s00330-021-08424-5>
11. Shirasaka T, Nagao M, Yamasaki Y, Kojima T, Kondo M, Hamasaki H, Kamitani T, Kato T, Asayama Y (2020) Low Radiation Dose and High Image Quality of 320-Row Coronary Computed Tomography Angiography Using a Small Dose of Contrast Medium and Refined Scan Timing Prediction. *J Comput Assist Tomogr* 44:7-12. <https://10.1097/RCT.0000000000000951.org/10.1097/RCT.0000000000000951>
12. Jia CF, Zhong J, Meng XY, Sun XX, Yang ZQ, Zou YJ, Wang XY, Pan S, Yin D, Wang ZQ (2019) Image quality and diagnostic value of ultra low-voltage, ultra low-contrast coronary CT angiography. *Eur Radiol* 29:3678-3685. <https://10.1007/s00330-019-06111-0.org/10.1007/s00330-019-06111-0>
13. Albrecht MH, Nance JW, Schoepf UJ, Jacobs BE, Bayer RR, 2nd, Litwin SE, Reynolds MA, Otani K, Mangold S, Varga-Szemes A, De Santis D, Eid M, Apfaltrer G, Tesche C, Goeller M, Vogl TJ, De Cecco CN (2018) Diagnostic accuracy of low and high tube voltage coronary CT angiography using an X-ray tube potential-tailored contrast medium injection protocol. *Eur Radiol* 28:2134-2142. <https://10.1007/s00330-017-5150-z.org/10.1007/s00330-017-5150-z>
14. Wang M, Fan J, Shi X, Qin L, Yan F, Yang W (2022) A deep-learning reconstruction algorithm that improves the image quality of low-tube-voltage coronary CT angiography. *Eur J Radiol* 146:110070. <https://10.1016/j.ejrad.2021.110070.org/10.1016/j.ejrad.2021.110070>
15. Wang Y, Zhan H, Hou J, Ma X, Wu W, Liu J, Gao J, Guo Y, Zhang Y (2021) Influence of deep learning image reconstruction and adaptive statistical iterative reconstruction-V on coronary artery calcium quantification. *Ann Transl Med* 9:1726. <https://10.21037/atm-21-5548.org/10.21037/atm-21-5548>
16. Wang H, Wang R, Li Y, Zhou Z, Gao Y, Bo K, Yu M, Sun Z, Xu L (2022) Assessment of Image Quality of Coronary Computed Tomography Angiography in Obese Patients by Comparing Deep Learning Image Reconstruction With Adaptive Statistical Iterative Reconstruction Veo. *J Comput Assist Tomogr* 46:34-40. <https://10.1097/RCT.0000000000001252.org/10.1097/RCT.0000000000001252>
17. Benz DC, Benetos G, Rampidis G, von Felten E, Bakula A, Sustar A, Kudura K, Messerli M, Fuchs TA, Gebhard C, Pazhenkottil AP, Kaufmann PA, Buechel RR (2020) Validation of deep-learning image reconstruction for coronary computed tomography angiography: Impact on noise, image quality and diagnostic accuracy. *J Cardiovasc Comput Tomogr* 14:444-451. <https://10.1016/j.jcct.2020.01.002.org/10.1016/j.jcct.2020.01.002>

18. Benz DC, Grani C, Mikulicic F, Vontobel J, Fuchs TA, Possner M, Clerc OF, Stehli J, Gaemperli O, Pazhenkottil AP, Buechel RR, Kaufmann PA (2016) Adaptive Statistical Iterative Reconstruction-V: Impact on Image Quality in Ultralow-Dose Coronary Computed Tomography Angiography. *J Comput Assist Tomogr* 40:958-963. <https://10.1097/RCT.0000000000000460.org/10.1097/RCT.0000000000000460>
19. Apfaltrer G, Szolar DH, Wurzinger E, Takx RA, Nance JW, Dutschke A, Tschauer S, Loewe C, Ringl H, Sorantin E, Apfaltrer P (2017) Impact on Image Quality and Radiation Dose of Third-Generation Dual-Source Computed Tomography of the Coronary Arteries. *Am J Cardiol* 119:1156-1161. <https://10.1016/j.amjcard.2016.12.028.org/10.1016/j.amjcard.2016.12.028>
20. Andreini D, Pontone G, Mushtaq S, Conte E, Perchinunno M, Guglielmo M, Volpato V, Annoni A, Baggiano A, Formenti A, Mancini ME, Beltrama V, Ditali V, Campari A, Fiorentini C, Bartorelli AL, Pepi M (2017) Atrial Fibrillation: Diagnostic Accuracy of Coronary CT Angiography Performed with a Whole-Heart 230-microm Spatial Resolution CT Scanner. *Radiology* 284:676-684. <https://10.1148/radiol.2017161779.org/10.1148/radiol.2017161779>
21. Chen Y, Wei D, Li D, Liu Z, Hu Z, Li M, Jia Y, Yu Y, Han D, Ren R, Yu N, He T (2018) The Value of 16-cm Wide-Detector Computed Tomography in Coronary Computed Tomography Angiography for Patients With High Heart Rate Variability. *J Comput Assist Tomogr* 42:906-911. <https://10.1097/RCT.0000000000000787.org/10.1097/RCT.0000000000000787>
22. Cherukuri L, Birudaraju D, Kinninger A, Chaganti BT, Pidikiti S, Pozon RG, Pozon ACG, Lakshmanan S, Dahal S, Hamal S, Flores F, Christopher D, Andreini D, Pontone G, Conte E, Nakanishi R, O'Rourke R, Hamilton-Craig C, Nasir K, Roy SK, Mao SS, Budoff MJ (2021) Use of Advanced CT Technology to Evaluate Left Atrial Indices in Patients with a High Heart Rate or with Heart Rate Variability: The Converge Registry. *J Nucl Med Technol* 49:65-69. <https://10.2967/jnmt.120.253781.org/10.2967/jnmt.120.253781>
23. Liang J, Wang H, Xu L, Yang L, Dong L, Fan Z, Wang R, Sun Z (2017) Diagnostic performance of 256-row detector coronary CT angiography in patients with high heart rates within a single cardiac cycle: a preliminary study. *Clin Radiol* 72:694 e697-694 e614. <https://10.1016/j.crad.2017.03.004.org/10.1016/j.crad.2017.03.004>
24. Miller RJH, Eisenberg E, Friedman J, Cheng V, Hayes S, Tamarappoo B, Thomson L, Berman DS (2019) Impact of heart rate on coronary computed tomographic angiography interpretability with a third-generation dual-source scanner. *Int J Cardiol* 295:42-47. <https://10.1016/j.ijcard.2019.07.098.org/10.1016/j.ijcard.2019.07.098>
25. Willeminck MJ, Noel PB (2019) The evolution of image reconstruction for CT-from filtered back projection to artificial intelligence. *Eur Radiol* 29:2185-2195. <https://10.1007/s00330-018-5810-7.org/10.1007/s00330-018-5810-7>
26. Park CJ, Kim KW, Lee HJ, Kim MJ, Kim J (2018) Contrast-Enhanced CT with Knowledge-Based Iterative Model Reconstruction for the Evaluation of Parotid Gland Tumors: A Feasibility Study. *Korean J Radiol* 19:957-964. <https://10.3348/kjr.2018.19.5.957.org/10.3348/kjr.2018.19.5.957>

Figures

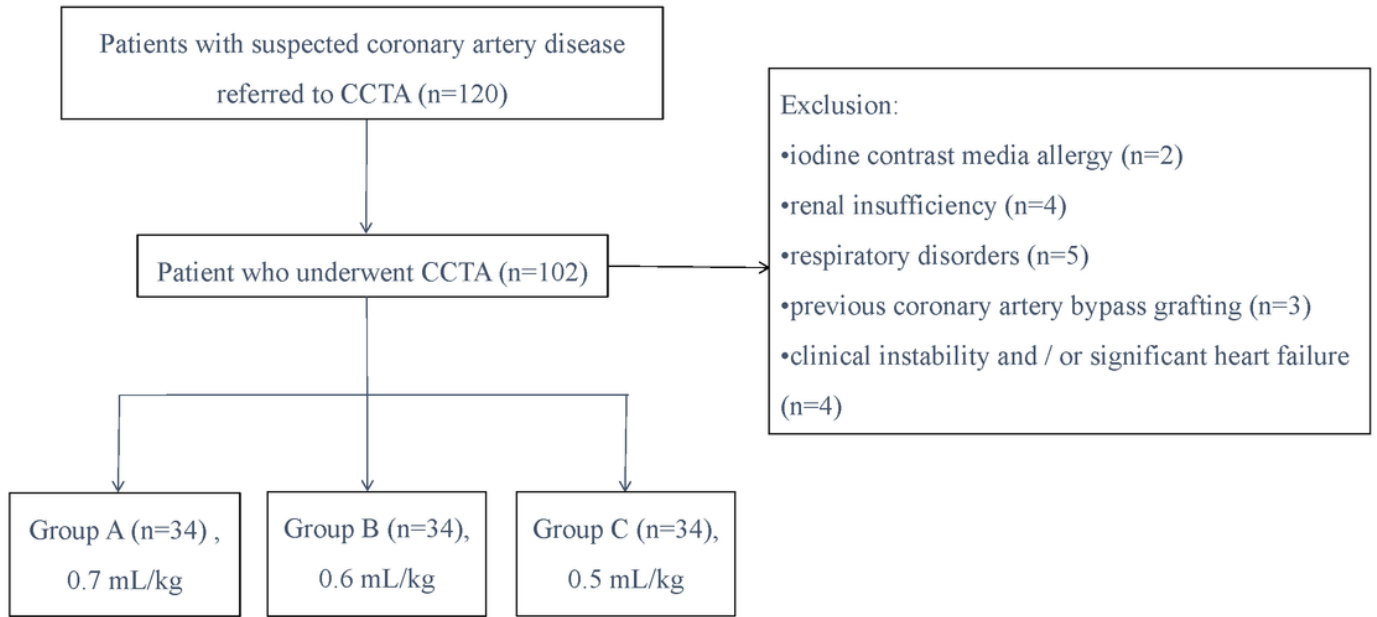


Figure 1

Study flowchart.

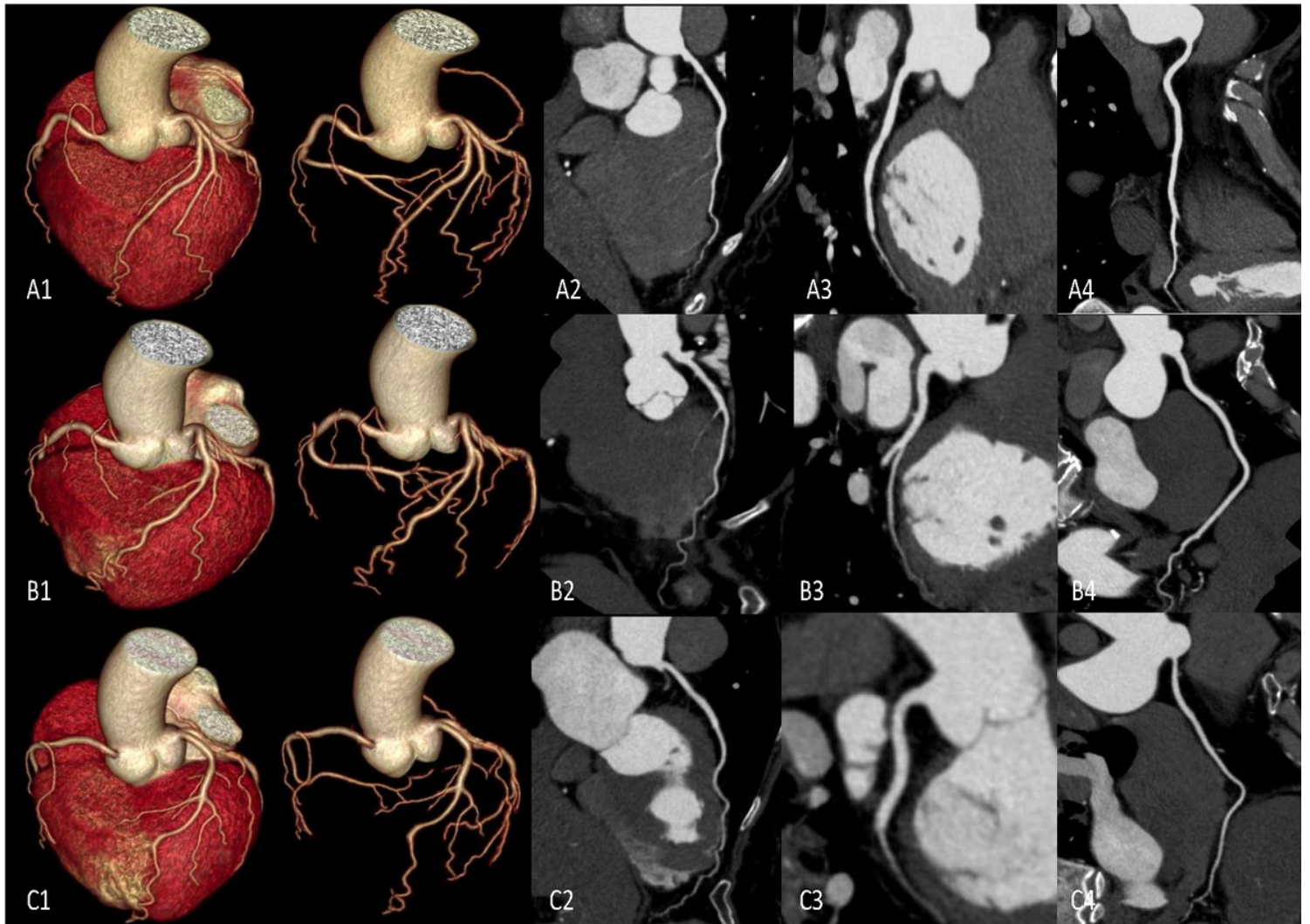


Figure 2

Image quality comparison among three groups. A1–A4, case in the Group A. Female, 57 years of age with BMI of 22.37 kg/m² and heart rate = 63 bpm. Attenuation in LAD, LCX, and RCA were 431 HU, 434 HU and 446 HU; B1–B4, case in the Group B. Female, 56 years of age with BMI of 22.89 kg/m² and heart rate = 61 bpm. Attenuation in LAD, LCX, and RCA were 428 HU, 424 HU and 441HU; C1–C4, case in the Group C. Female, 56 years of age with BMI of 23.44 kg/m² and heart rate = 58 bpm. Attenuation in LAD, LCX, and RCA were 421 HU, 419 HU and 437HU. The image quality of these patients all reached subjective scores of 5 with clear border of the blood vessels and excellent diagnostic performance.

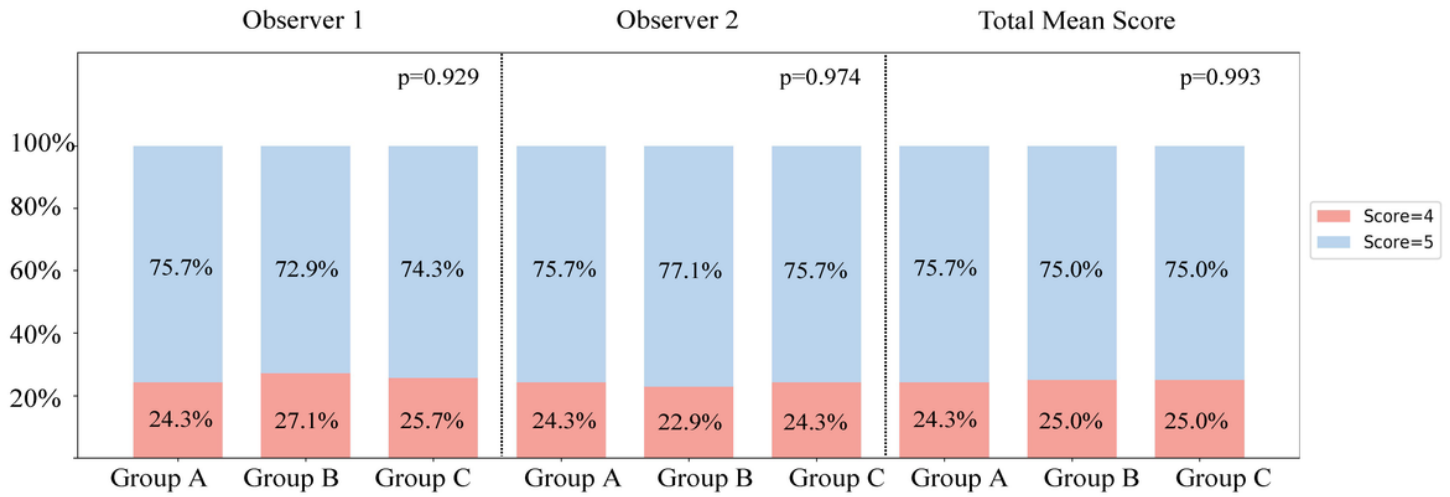
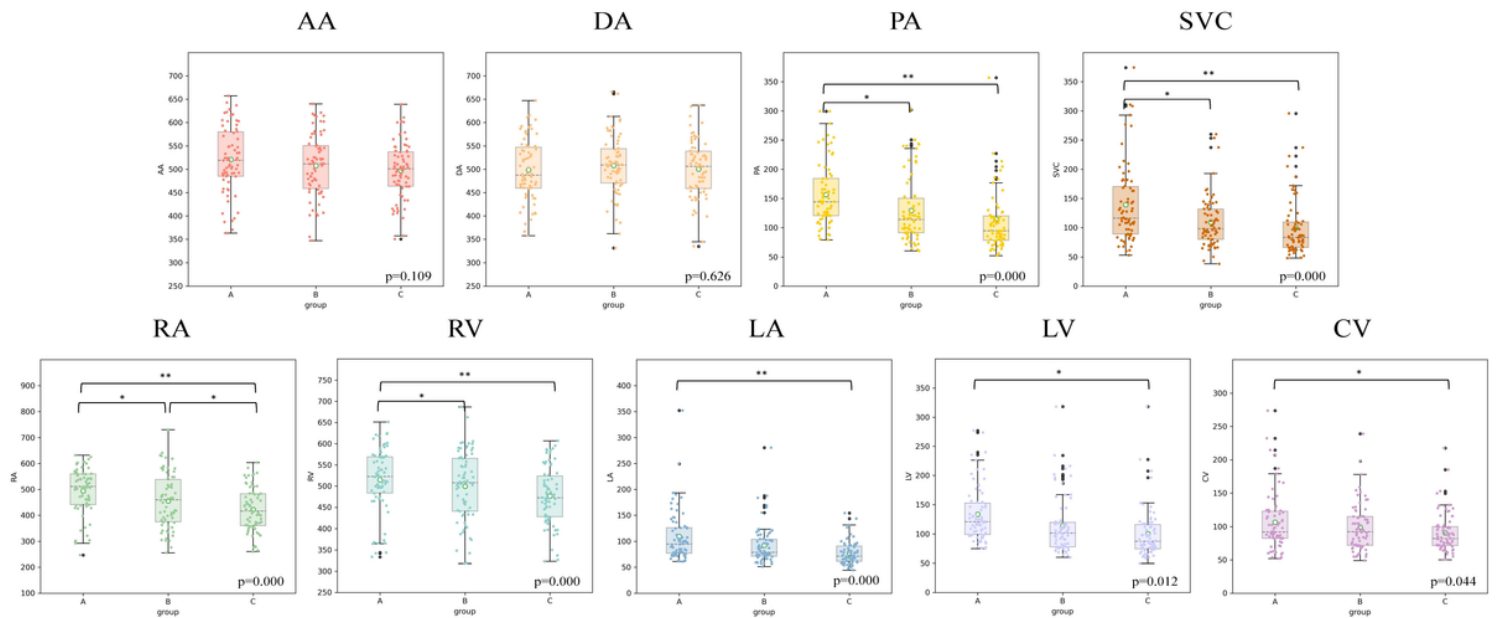


Figure 3

Subjective image quality evaluation from two observers. The difference in subjective image quality rating between two observers never exceeded one point, and their evaluations reached a Cohen's kappa of 0.796 (95% CI: 0.700-0.892).



* $p < 0.05$ ** $p < 0.001$

Figure 4

Box-plot comparison of CT values for ascending aorta (AA), descending aorta (DA), pulmonary artery (PA), Superior vena cava (SVC), right atrium (RA), right ventricle (RV), left atrium (LA), left ventricle (LV) and coronary vein (CV) among three groups.

* Indicates range of P values: * $p < 0.05$; ** $p < 0.001$

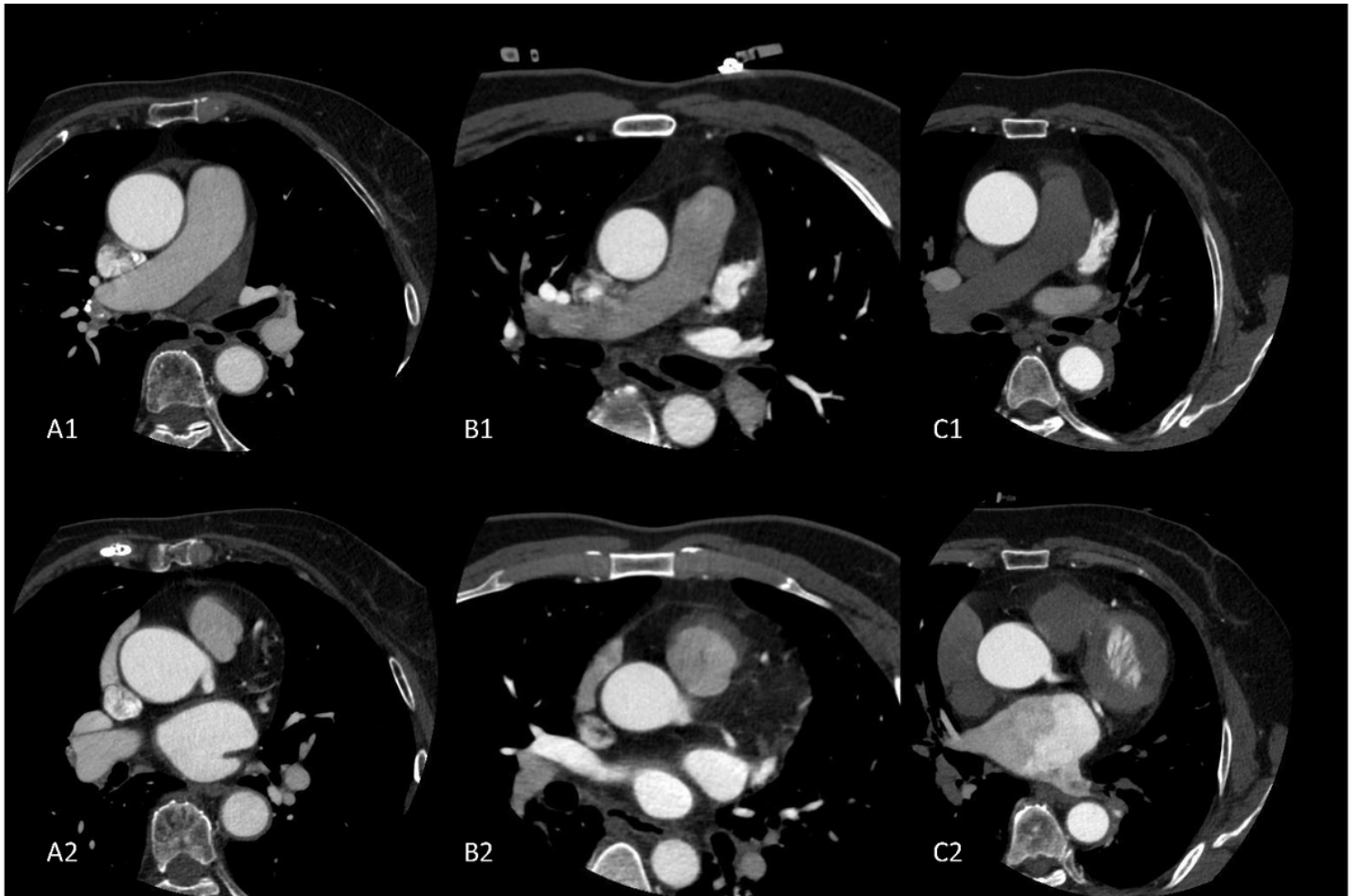


Figure 5

Comparison of the quality of axial images in the three groups. A1-A2, Group A cases, female, 58 years old, body mass index 30.22 kg/m^2 , heart rate 77 bpm; B1-B2, Group B cases. Female, 52 years old, BMI 29.45 kg/m^2 , heart rate 71 bpm; C1-C2, Group C cases, female, 60 years old, BMI 29.67 kg/m^2 , heart rate 68 bpm. The A1, B1, C1 images are all at the level of the right main trunk of the pulmonary artery, and the A2, B2, C2 images are all at the level of the left main trunk of the coronary artery, and it can be seen that the excessive amount of contrast deposited in the superior vena cava in the images of Groups A and B, which produces scattering artefacts and reduces the image quality. But this does not exist in Group C, which shows that Group C protocol can provide adequate enhancement in coronary arteries and do not produce contrast redundancy.

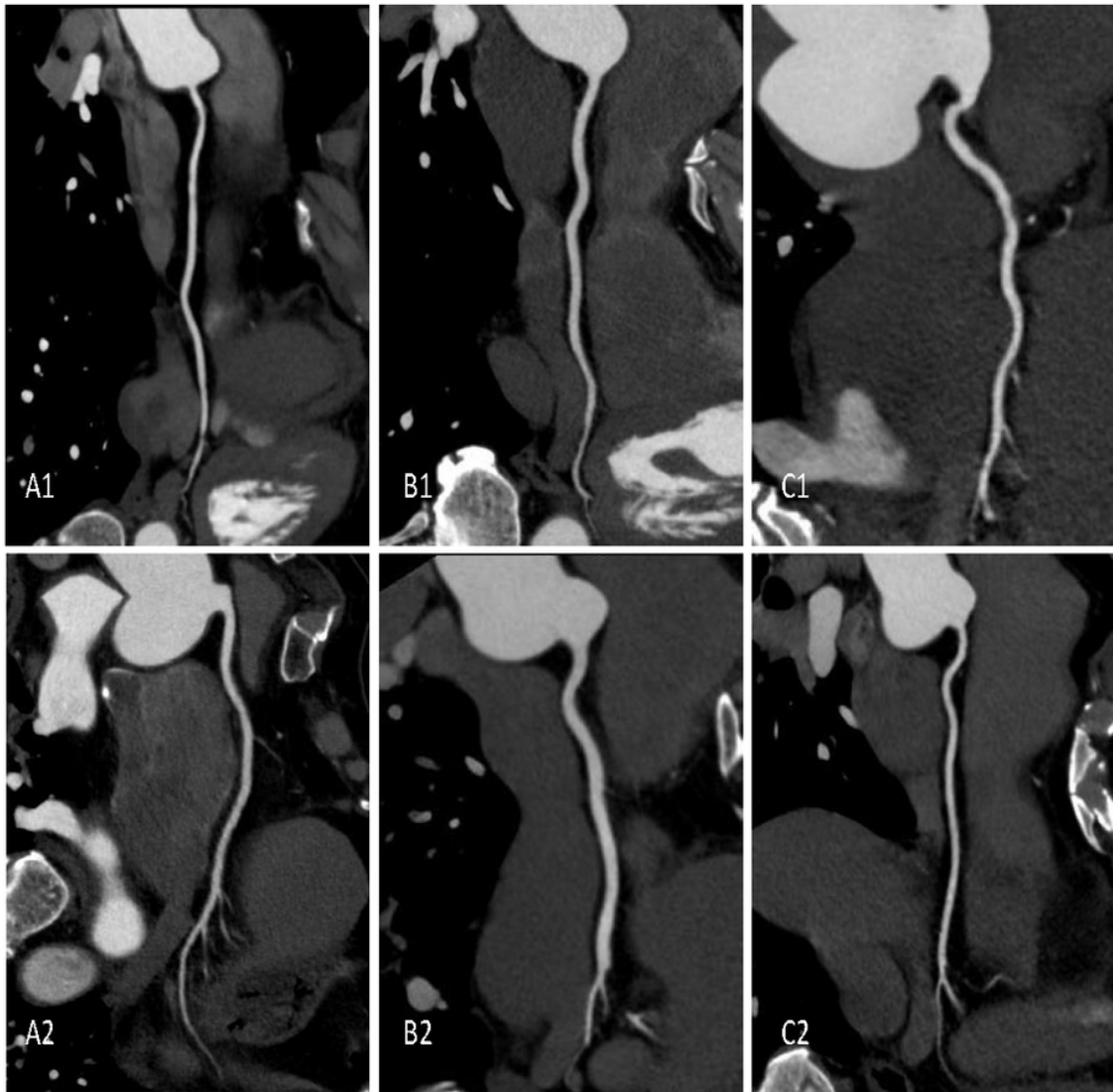


Figure 6

Image comparison for subgroup analysis. A1–A2, case in the Group A. A1, a male in low HR group, 55 years of age with BMI of 24.11 kg/m² and heart rate = 62 bpm. A2, a male in high HR group, 58 years of age with BMI of 24.09 kg/m² and heart rate = 83 bpm; B1–B2, case in the Group B. B1, a male in low HR group, 51 years of age with BMI of 24.62 kg/m² and heart rate = 54 bpm. B2, a male in high HR group, 57 years of age with BMI of 24.49 kg/m² and heart rate = 71 bpm; C1–C2, case in the Group C. C1, a male in low HR group, 55 years of age with BMI of 24.57 kg/m² and heart rate = 53 bpm. C2, a male in high HR group, 59 years of age with BMI of 24.15 kg/m² and heart rate = 72 bpm. The low-contrast dose protocol in this study can be applied to both low HR heart rate and high HR patients.

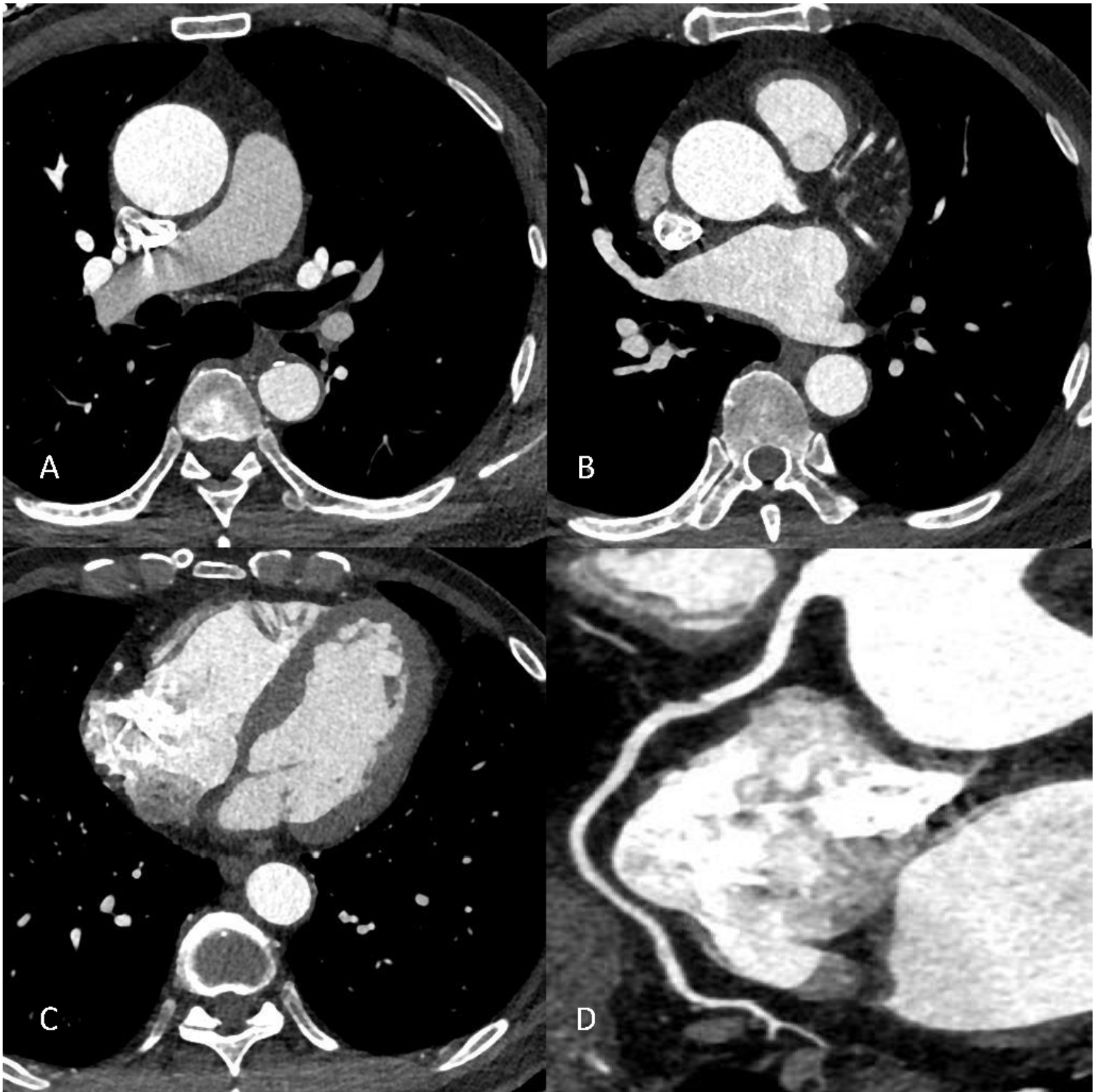


Figure 7

Typical case of group A. Male, 65 years old, body mass index 24.61kg/m², heart rate 79 bpm. The image A is at the level of the right main trunk of the pulmonary artery, and image B is at the level of the left main trunk of the coronary artery, image C is at the level of the middle portions of the right coronary artery and image D shows the CPR image of right coronary artery. In this case, images A, B show that excessive contrast retention in the superior vena cava resulted in high vascular attenuation values and reduces image quality;

images C, D show that contrast redundancy in the right atrium leads to scattering artefacts that interfere with the diagnosis of the right coronary artery.